

The Role of Interfacial Molecular Structure in the Adsorption of Ions at the Liquid–Liquid Interface

Cathryn L. McFearn and Geraldine L. Richmond*

Department of Chemistry, University of Oregon, Eugene, Oregon 97403

Received: July 13, 2009; Revised Manuscript Received: October 30, 2009

One of the most common and important interfaces is the boundary layer between an aqueous phase solution of ions and a hydrophobic medium. Whether the hydrophobic medium is a membrane, a macromolecular assembly, or a simple organic liquid, our molecular-level understanding of how ions in an adjacent aqueous phase approach, alter, and transport across the boundary is still quite deficient, largely due to experimental challenges in making the appropriate measurements. This paper reports some of the first measurements of the behavior of common inorganic ions at the interface between different aqueous phase salt solutions (NaCl, NaBr, NaNO₃, and Na₂SO₄) and a hydrophobic organic liquid (CCl₄). The results show that the ions reside within the interfacial region where they affect the water hydrogen bonding in a manner specific to the ion under study. Distinct differences in the behavior of ions at this interface relative to the air–water interface are found and discussed.

Introduction

Accompanying the expanding interest in the behavior of water at hydrophobic surfaces is the question of how this interfacial behavior might be altered by the presence of small, inorganic ions in an adjacent aqueous phase. This is a particularly important question when the hydrophobic medium is fluid in nature and, as a result, is semipermeable to neighboring water molecules and ions. The interplay between interfacial water, ions, and the organic liquid lies at the heart of some of the most important environmental and biological processes that occur on this planet including ion transport, environmental remediation, and phase transfer catalysis. The complex interactions present at such interfaces are controlled by a combination of forces that vary in strength, which we are only beginning to understand through emerging experimental^{1–10} and computational approaches.^{11–20}

The studies presented herein focus specifically on understanding the interfacial molecular interplay between an aqueous ionic solution in contact with the hydrophobic liquid carbon tetrachloride (CCl₄). These experimental studies that measure vibrational spectra of the interfacial water molecules using vibrational sum-frequency spectroscopy (VSFS) show how ions behave differently at this organic–water interface relative to ions at the air–water interface.^{21–31} The results also provide further insight into how the characteristics of particular ions, such as charge and solvation, play a role in how water molecules bond and orient near their organic interfacial counterparts. These studies build on the knowledge base of over a decade of studies in our laboratory of the molecular behavior of water at neat organic–water interfaces,^{8,9} and at air–water interfaces with ions present.^{28,30,31} They also confirm some of the ideas and concepts that have emerged from our previous molecular dynamics (MD) simulations^{15,16} regarding how weak organic–water interactions might play a role in how ions structure and transport across such interfaces.

VSFS Background. Detailed explanations of VSFS can be found in the literature so it will only briefly be described here.^{32–34} In these VSFS experiments a laser beam with a fixed visible frequency (ω_{vis}) is overlapped both spatially and temporally with a tunable infrared (IR) beam (ω_{IR}) at the interface generating a resulting beam at the sum of these two frequencies (ω_{SF}). Under the electric dipole approximation, this beam, ω_{SF} , is only generated by those molecules or collection of molecules that create a noncentrosymmetric environment, such as at the CCl₄–water boundary. This results in no significant contribution to VSFS signal from the bulk liquid molecules leading to inherent interface specificity. It also means the probe depth on either side of the interface is limited to the narrow interfacial region that possesses a net average molecular orientation of water or CCl₄.

The intensity $I(\omega_{\text{SF}})$ of the VSFS light generated at the interface is given by

$$I(\omega_{\text{SF}}) \propto |\chi^{(2)}|^2 I(\omega_{\text{IR}}) I(\omega_{\text{vis}}) \quad (1)$$

where $I(\omega_{\text{IR}})$ and $I(\omega_{\text{vis}})$ are the respective intensities of the incoming tunable infrared and visible beams and $\chi^{(2)}$ is the macroscopic second order nonlinear susceptibility. $\chi^{(2)}$ is composed of a nonresonant term, $\chi_{\text{NR}}^{(2)}$, and a resonant term, $\chi_v^{(2)}$. $\chi_{\text{NR}}^{(2)}$ is observed to be negligible for the current experiments. The resonant term can be written as

$$\chi_v^{(2)} \propto \frac{NA_v}{\omega_v - \omega_{\text{IR}} - i\Gamma_v} \quad (2)$$

where N is the number density of molecules, A_v is the product of the Raman and IR transition moments, ω_v is the vibrational transition frequency, ω_{IR} is the tunable IR frequency, and Γ_v is the line width of the transition. Generally these susceptibility terms are complex quantities that have both phases and amplitudes, giving rise to VSFS intensity that is proportional to the square of the sum of the terms. The resulting spectrum can have either constructive or destructive interferences between contributions from different interfacial modes.

* To whom correspondence should be addressed. Phone: (541)346-4635. Fax: (541) 346-5859. E-mail: richmond@uoregon.edu.

The macroscopic term $\chi_v^{(2)}$ is related to the microscopic property, the molecular hyperpolarizability β , by the following equation via the number density of the molecules probed, N , and their orientation.

$$\chi_v^{(2)} = \frac{N}{\epsilon_0} \langle \beta \rangle \quad (3)$$

The angular brackets denote an ensemble average over different molecular orientations. By choosing different polarization combinations, different elements of the $\chi_v^{(2)}$ tensor are probed. All spectra that are shown in this work were taken in the *ssp* polarization combination (s-SF, s-visible, p-IR), which probes the $\chi_{yyz}^{(2)}$ element and consequently those vibrational modes that have a component of their transition dipole perpendicular to the interfacial plane.

Experimental Section

The laser system used in these experiments is a commercially available VSFS system purchased from Ekspla (Vilnius, Lithuania). It is pumped by a Nd:YAG laser (model PL2143A: ~ 30 ps, 10 Hz). A portion of the 1064 nm fundamental output is sent through a Potassium Dideuterium Phosphate (K*DP) crystal where it is frequency doubled to generate 532 nm light. Part of this 532 nm light is focused and sent to the sample cell as the visible portion (ω_{vis}) to generate the VSFS signal. The remaining 532 nm light, in addition to the 1064 nm light not frequency doubled, is used in a series of nonlinear optical processes (model PG501/DFG2-10P) to generate the tunable IR light. Beam energies used in the current experiments are 80 μJ and ~ 200 –250 μJ for the visible and IR beams, respectively. The 532 nm visible and tunable IR beams are overlapped at the liquid–liquid interface in a total internal reflection (TIR) geometry to maximize the VSFS signal intensity. The beam sizes at the interface are estimated to be ~ 1 mm for both the visible and IR beams. Beam angles to achieve this geometry were chosen to maintain TIR of the visible beam for all concentrations of all the salts used in the aqueous solution: 69.5° and 75° from the interface normal for the visible and IR beams, respectively. To separate the reflected visible light from the generated VSF beam, two RazorEdge filters (Semrock) and one holographic notch filter (Kaiser Optical) are employed. The remaining VSF light is focused by an anti-reflective coated BK7 lens and the polarization selected by a glan prism polarizer and half-waveplate, all part of the Ekspla system. The beam is then sent through a monochromator (model MS2001) and detected by a photomultiplier tube (Hamamatsu R7899). The liquid–liquid sample holder consists of an IR grade fused silica prism (purchased from Ekspla) clamped to a Kel-F cylinder and sealed by a Viton o-ring.

Multiple spectra of each interface were taken and averaged to achieve an acceptable signal-to-noise level. Spectra of the same salt solutions were taken on multiple days to ensure reproducibility. A neat CCl_4 –water spectrum was taken at the beginning and end of each day that salt solution data were collected in order to estimate fluctuations in intensity from day to day, as well as ensure no contamination effects.

The VSF spectral results were shown to be extremely sensitive to chemical impurities so great care was taken to eliminate any effects from these. CCl_4 ($\geq 99.9\%$ +, Chromosolv HPLC grade) was purchased from Sigma-Aldrich and then distilled twice before use in any experiments. All salts used were also purchased from Sigma-Aldrich (99.0% Sigma Ultra grade). Although a high grade purity, using the salts as purchased resulted in inconsistent spectral results as well as

peaks in the VSF spectra at ~ 2850 and 2900 cm^{-1} indicating the presence of organic, surface active impurities. The salts were therefore baked in an oven at 220°C for ~ 12 h prior to use. Although this temperature is lower than that used by other researchers^{35–37} (range from ~ 400 to 650°C) for purification in past salt investigations by VSFS, it was sufficient to remove the organic impurities. The resulting spectra were very consistent and free of any peaks in the CH stretching region. Water used in these experiments came from a Nanopure II filtering system (Barnstead) with an $18\text{ M}\Omega\cdot\text{cm}$ resistivity. Fresh salt solutions were prepared every day of data collection. All glassware used in addition to the sample cell components were cleaned in NoChromix dissolved in concentrated sulfuric acid, and then rinsed copiously with the Nanopure filtered water. Due to lower aqueous solubility at room temperature, the Na_2SO_4 solutions were sonicated prior to use.

Results and Discussion

To aid in the discussion of the interpretation of the ionic solution spectra, a brief overview of the general features for the neat CCl_4 –water spectrum is given below. These general features are common to most of the organic–water interfacial systems studied thus far in our laboratory.^{8,9} The neat spectrum of this interface is shown in Figure 1 by the black traces. It is comprised of water OH stretch modes that are highly sensitive in both their frequencies and spectral breadths to their local hydrogen bonding environment. As in linear vibrational spectroscopies, the greater the degree of hydrogen bonding character a collection of water molecules possesses, the lower the stretching frequency will be. Due to the homogeneous and inhomogeneous broadening resulting from the condensed phase interface, in addition to the complicated lineshapes resulting from VSF spectral interferences, analysis and assignment of spectral features proves challenging. The interpretation of the CCl_4 –water spectrum given below is thus a result of a combination of efforts consisting of both past spectral fitting^{38,39} and more recent MD analyses^{40,41} that provide a comprehensive understanding and view of the interface that will be applied to the interpretation of the results to follow. A cartoon representing this interpretation of the interface and accompanying hydrogen bonding environment is shown in Figure 2.

In general, water molecules at the CCl_4 –water interface are highly oriented. This is most evident by the presence of the sharp, intense spectral feature near 3665 cm^{-1} that corresponds to one of the uncoupled OH stretch modes of water molecules that “straddle” the interface (labeled I in Figure 2). The OH oscillator from these water molecules, referred to as the “free OH”, is oriented into the CCl_4 phase to which it very weakly bonds. Its frequency has been found to be a sensitive indicator of weak water–organic bonding interactions for different liquid–liquid systems.^{8,9} Due to the geometry of these straddling water molecules, their companion OH oscillators are necessarily oriented toward the aqueous phase. These OH oscillators can act as hydrogen bond donors to other water molecules deeper within the interfacial region and are thus referred to as the “donor OH” modes (labeled II in Figure 2). The broad spectral region in the CCl_4 –water spectrum around 3500 cm^{-1} is attributed to these oscillators. The assignment of this spectral region, based initially on isotopic dilution experiments,³⁸ has been more recently confirmed by computational VSF spectra generated from MD simulations⁴⁰ following the work of Morita and Hynes.⁴² These simulations show this intramolecularly uncoupled OH mode is bonded to two nearby water molecules through its H and O atoms and appears in this spectral region

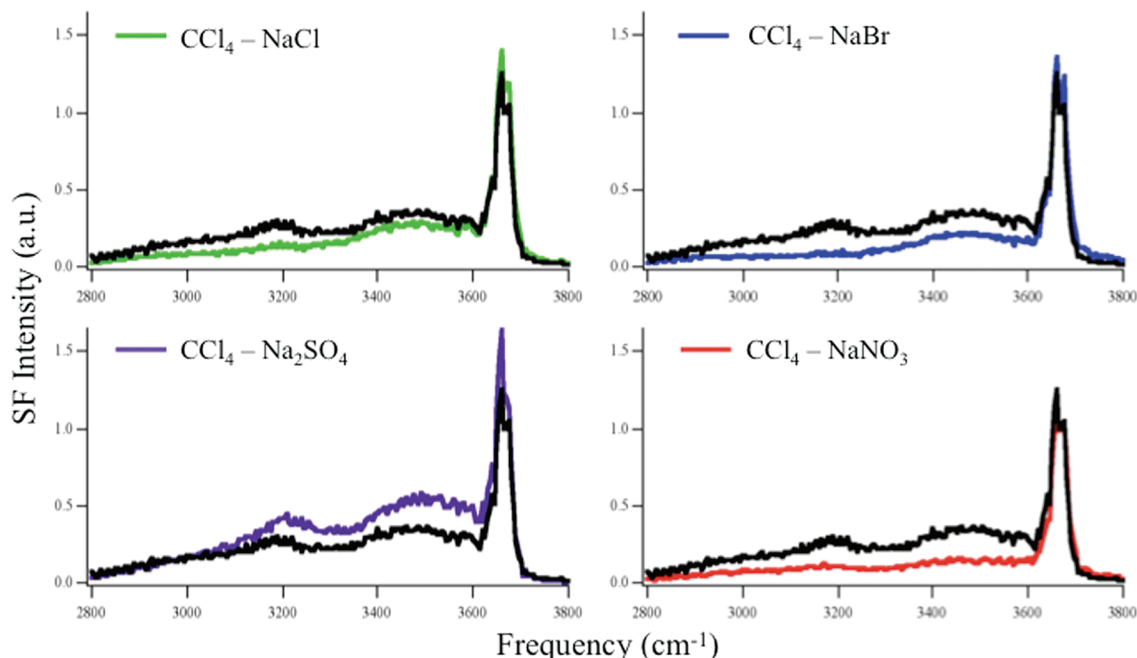


Figure 1. VSF spectra of the $\text{CCl}_4\text{--NaX(aq)}$ interface at 1.2 M: $\text{X} = \text{Cl}^-$ (green), Br^- (blue), NO_3^- (red), SO_4^{2-} (purple). The black trace in each panel shows the neat $\text{CCl}_4\text{--water}$ interface spectrum for comparison.

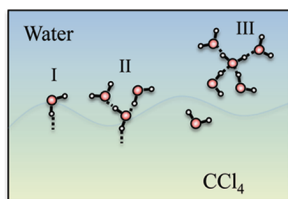


Figure 2. Cartoon of the $\text{CCl}_4\text{--water}$ interfacial bonding environment: (region I) straddling water molecule with a free OH oscillator residing at the top layer of the interface; (region II) straddling water molecule with free OH and donor OH oscillators; and (region III) water molecules found deeper within the interfacial region with greater hydrogen bonding character. Dashed lines designate bonding interactions.

along with other minor contributions from this uncoupled OH mode bonded to neighboring water molecules through single or double electron donor bonds from its oxygen atom.

Because the water molecules containing these uncoupled OH free and donor bonds bridge the interface, they necessarily tend to reside in the topmost interfacial layer. Also, because the orientation of the transition moment of these bonds has a component in the plane perpendicular to the interface, their contributions dominate the intensity in the $3400\text{--}3700\text{ cm}^{-1}$ region under the *ssp* polarization scheme. Also contributing to the overall VSF spectrum, but at lower frequencies, are water molecules that form a network of more and stronger hydrogen bonds to neighboring water molecules. Their spectral contributions appear in the lower frequency region of the spectrum below $\sim 3400\text{ cm}^{-1}$, characteristic of stronger hydrogen bonded species. Our experimental observations and computational results indicate that the oriented water molecules contributing to this spectral region mainly reside one or two molecular layers deeper in the interfacial region than those described above with weaker bonding character.^{41,43} The structure of molecules in the spectral region around 3200 cm^{-1} is of the strongest bonding character and is often referred to, in a simplistic manner, as water molecules with tetrahedral bonding due to the similar vibrational spectral peaks found in spectra of ice. These oriented and more strongly hydrogen bound water molecules, represented in Figure

2 by region III, tend to reside deeper in the interfacial region and are less prevalent at this interface. Also contributing to this spectral region are a multitude of water molecules with relatively strong hydrogen bonding interactions but with more asymmetric bonding character than the tetrahedral picture.⁴⁰

Figure 1 presents spectra of 1.2 M NaX ($\text{X} = \text{Cl}^-$, Br^- , NO_3^- , SO_4^{2-}) solutions at the interface with CCl_4 along with comparative spectra of the neat $\text{CCl}_4\text{--water}$ interface. In each case the spectra of the different salt solutions differ markedly from each other and from the neat $\text{CCl}_4\text{--water}$ spectrum. The presence of the monovalent ions (Cl^- , Br^- , NO_3^-) results in a measurable decrease in intensity below $\sim 3600\text{ cm}^{-1}$ with little to no change in the intensity of the free OH mode. However, the degree of intensity decrease differs for each anion containing solution. For the $\text{CCl}_4\text{--NaCl(aq)}$ interface (green), the presence of the ions causes a measurable decrease in intensity in the 3200 cm^{-1} region along with a somewhat smaller but significant decrease in the region where donor OH bonds dominate (3500 cm^{-1}). For the NaBr containing solution (blue), the decrease in the donor OH spectral region is overall greater than that for the NaCl solution. The decrease in this region is even larger for the NaNO_3 containing system (red), reduced to relatively low resonant intensity in this spectral region at this concentration. The presence of Na_2SO_4 has a very different effect. Unlike the monovalent ion containing solutions, the spectrum of the $\text{CCl}_4\text{--Na}_2\text{SO}_4\text{(aq)}$ interface (purple) shows a significant enhancement in the intensity throughout the strong and weakly water bonded regions.

The effect of bulk salt concentration on the VSFS intensities in three spectral regions is given in Figure 3. These were determined by plotting the intensity at each wavelength (3200 , 3500 , and free OH = 3665 cm^{-1}) versus bulk salt concentration. Beginning with the monovalent ions, the reduction in intensity in the strongly bonded 3200 cm^{-1} region is similar for all ions at each of the concentrations (Figure 3a). In contrast, the intensities for the three different monovalent ions are more highly concentration dependent for the donor OH spectral region (Figure 3b), with NO_3^- showing the greatest decrease followed

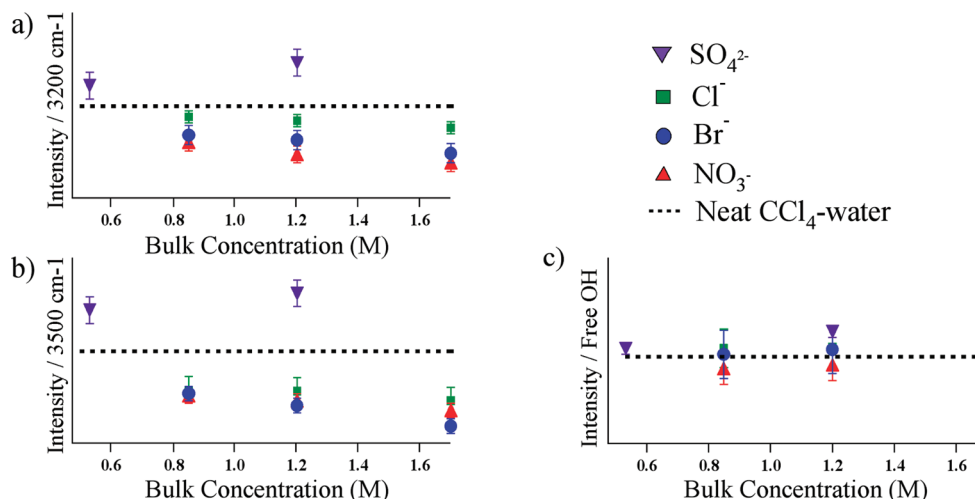


Figure 3. VSFS intensity versus bulk salt concentration (M) for the spectral regions at (a) 3200 cm⁻¹, (b) 3500 cm⁻¹, and (c) free OH. The horizontal, dashed lines represent the value for the neat CCl₄–water interface spectrum.

by Br⁻ and Cl⁻. For the SO₄²⁻ spectra, the concentration range is smaller and only composed of two data points due to limits of solubility. However, the trend is still apparent that upon addition of Na₂SO₄ both spectra show an increase in intensity for both spectral regions. Figure 3c shows the concentration dependence of the free OH intensity. In contrast to the clear concentration dependent trends seen for the other spectral regions, the free OH exhibits no significant change within experimental error with the addition of these added salts.

Figures 1 and 3 clearly show that the addition of ions to the aqueous phase causes distinct changes in the water bonding character in the interfacial region of these salt solutions adjacent to liquid CCl₄. Although the ions themselves are not being probed spectroscopically, the changes in the different regions of the OH stretching spectrum convey unique information about what is happening within the interface. The most definitive conclusion that can be drawn is that there are, for this organic–water interface, ions present in the interfacial region. This is a particularly important determination, given the general evolving picture of ion behavior at aqueous interfaces that has arisen since the initial MD simulations of ions at the air–water interface conducted by Jungwirth and Tobias.⁴⁴

For all the spectra shown in Figure 1, the common cation was Na⁺. To examine the role of the cation on the structure of the water, VSF spectra of solutions with the same anions were made substituting K⁺ for Na⁺ as the counterion (not shown). The spectra of the same concentration and the same anion show the same trends, indicating that the anion, and not the cation, primarily causes the alteration in the interfacial spectra for these cations being probed. We conclude that for this particular organic–water interface, the presence of the cations either does not affect the water structure as much as the anions, or they are at a lower concentration at the topmost interfacial depths within this thin interfacial region. The latter is consistent with MD simulation of ions at organic–water interfaces.²⁰ Layering of the positive and negative charges within the interface can also lead to net polarization causing spectral changes. No change to the spectra by varying the cation also suggests little ability of the cations to alter the ions' spatial distributions throughout the interface.

Because the use of bulk molar concentrations of salts in the present experiments can slightly alter the pH of the solution, the effect of pH on the spectra was also examined at acid/base concentrations relevant to this study. Alteration of the pH in

this range (pH ~6–8) did not affect the results described above for the salts examined. More extensive studies of acidic and basic solutions at the interface with CCl₄ will appear in a later publication. It should also be noted that because the spectra of Na₂SO₄ were acquired under higher ionic strength conditions than the other salts studied, the effect of ionic strength on the spectra was explored by holding it constant with excess NaCl (spectra not shown). Lack of detectable differences in the spectra were observed, indicating that the ionic strength does not affect the structure of the interfacial water molecules at these high ion concentrations. This further emphasizes that the resulting differences in the spectra are due to the specific anion being studied.

The presence of these ions in the interfacial region clearly alters the way interfacial water molecules behave as manifested in these spectral changes. From eqs 2 and 3 it is apparent the two contributing factors for these intensity changes are (1) a change in the number of contributing water bonded species in their corresponding spectral region and (2) a change in orientation of various water bonded species. The former effect comes from the fact that VSFS intensity is proportional to the square of the number density, N . The latter arises from the dependence of the VSFS response on molecular orientation through the molecular hyperpolarizability values, β , and consequently through $\chi_v^{(2)}$. When the water molecules are in a more random configuration, their dipoles will cancel to a certain degree leading to a lower value for the orientationally averaged β value and therefore a decrease in $\chi_v^{(2)}$.

For further insight into the molecular reasons behind the spectral trends, we draw on our knowledge base of ions at the air–water interface for which similar experiments have been conducted. What is observed here for the monovalent ions at the liquid–liquid interface is distinctly different than what we and other laboratories observe for these ions at the air–water interface using VSFS.^{28,29,45,46} This comparison is shown in Figure 4, which displays the VSF spectra of the CCl₄–NaX_(aq) (X = Cl⁻, Br⁻, and SO₄²⁻) interfaces with their analogous (similar bulk concentration regime) air–salt_(aq) spectra taken from previous studies done in our research group.^{28,31} For the case of air–water, the monovalent ions result in small changes in VSF intensity in the 3200 cm⁻¹ region, and almost negligible changes in the weaker bonded 3500–3600 cm⁻¹ region. Isotopic dilution studies from this laboratory further indicate that these small VSFS intensity changes due to the presence of Cl⁻ or

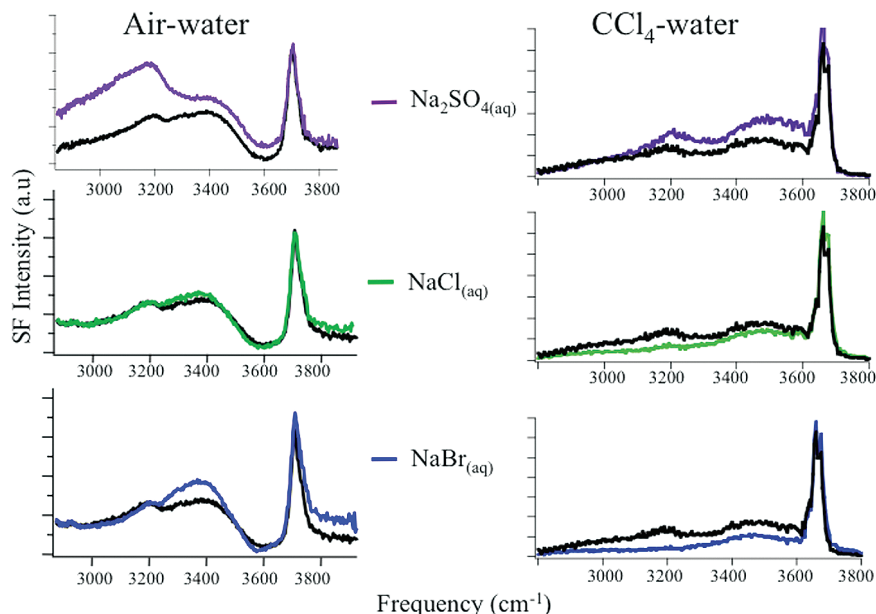


Figure 4. Comparison of air–NaX(aq) (left side) to CCl₄–NaX(aq) (right side) to VSF spectra for X = Cl[−] (green), Br[−] (blue), and SO₄^{2−} (purple). Neat spectra are shown in each panel by the black traces. The spectra for the air–water interfacial systems are adapted from refs 28 and 31.

Br[−] ions are a reflection of the alteration of water bonding deeper in the interfacial region where water bonding is stronger.²⁸ For the air–water interface the addition of salts has been attributed mostly to the ions widening the interfacial region further into the aqueous bulk water resulting in increased VSF spectral intensity,^{28,36,46} a picture consistent with computational efforts.^{22,23} The specific details as to the exact depths that the ions reside within the interface, the specific vibrational mode assignments and importance of certain water bonded species affected by the ions, and other factors such as coupling between vibrational modes are a matter of ongoing debate for the air–water interface.^{28,23,45,47,48} What consistently emerges from examination of all of these studies, however, is the clear difference in the behavior of ions at that air–water interface relative to the CCl₄–water interface where the ions significantly perturb both strong and weakly bonded water molecules, from the topmost to the deeper regions of the interface.

We conclude that this difference in ion behavior for these two interfaces is due to the unique nature of the organic–water interface that facilitates the adsorption of anions relative to the air–water boundary. All evidence from our experimental and computational efforts and others indicates that the neat CCl₄–water interface consists of water molecules with a relatively high degree of orientational ordering.^{16,41,49,50} This is true in particular for the topmost region of the interface where the water molecules adopt specific orientations due to their contact with the organic phase, in this case the non-polar liquid CCl₄. MD simulations conducted previously in our laboratory demonstrate that for the neat CCl₄–water interface, the CCl₄ also displays orientational layering near the interface, which extends several molecular layers into the organic phase.⁵¹ Later MD simulations by Hore et al. went further to suggest that the combination of the orientational ordering of the water and the organic would lead to an interfacial field across the boundary region that could have an influence on charged species in the aqueous phase.¹⁶ Figure 5 shows pictorially the direction of the field derived in the work that results from summing the overall net dipole of the water molecules in the direction normal to the interface.

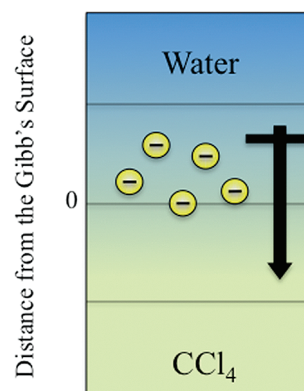


Figure 5. Cartoon of the electric field present at the organic liquid–water interface that promotes accumulation of ions in that region (adapted from ref 15). The dipole arrow uses the convention of pointing in the negative direction.

With this picture in mind, the effect that the presence of the different anions has on water in the topmost and slightly deeper regions of the interface is particularly interesting. If the accumulation of ions within the interface were simply an electrostatic effect, then all the monovalent ions should decrease the VSFS signal equally as they populate the interface and screen the field. This is what is observed in Figure 3a where by increasing the bulk salt concentration, the intensity around 3200 cm^{−1} decreases in a nearly identical manner for all the monovalent anions. As the interfacial field is screened by these ions, fewer of these more strongly bonded water molecules that reside deeper in the interface orient with the field, resulting in the reduction in VSF spectral response. This is the region most commonly found to exhibit effects due to a reduction in interfacial field.⁴³

The water molecules that reside more in the topmost interfacial region and undergo weaker bonding interactions show greater sensitivity to the characteristics of the different ions, and to a much higher degree than observed for the air–water interface. In this region, at a given concentration, the monovalent ions can be ranked according to their ability to decrease the

VSFS intensity in the 3500 cm^{-1} region as shown in Figure 3b: $\text{Cl}^- < \text{Br}^- < \text{NO}_3^-$. This trend follows the size of the ions, with Cl^- being the smallest and NO_3^- the largest. Cl^- is also the least polarizable with NO_3^- and Br^- calculated to have similar polarizabilities.^{23,52} We attribute these VSF spectral trends to the differences in the degrees of penetration of the ions into the topmost interfacial region, facilitated in part by the interfacial field. The higher polarizability of the larger ions results in their greater presence at the dividing surface and consequently a reduction in field, a narrower interfacial region, and a displacement of water molecules in the topmost water layers. The overall consequence of the presence of the ions, in particular the larger and more polarizable ones, is that water molecules within the weakly bonded interfacial region are displaced to a certain degree and are less highly oriented, both of which result in decreases of the VSFS intensity as shown in eqs 2 and 3, respectively.

The MD studies by Wick and Dang of halide ions at the CCl_4 –water interface also show that larger and more polarizable ions have a higher presence at this interface.²⁰ Their simulations also show that, for a given concentration, Br^- is found at a greater density at the air–water interface than at CCl_4 –water but Cl^- exists at roughly the same density at both the air–water and CCl_4 –water interfaces. That our VSFS studies presented here in Figure 4 show more drastic effects at CCl_4 –water than at air–water by the presence of these ions does not necessarily contradict the MD findings that Br^- and Cl^- reside at higher or equal concentration at air–water relative to CCl_4 –water. The differences lie primarily in the information being probed by the two methods.

Interfacial SO_4^{2-} also alters the water bonding character at the CCl_4 –water interface but in an opposite trend than is observed for the monovalent ions throughout the spectral region. We attribute this different behavior to the higher charge of the SO_4^{2-} ion causing it to have a more solvated nature. To remain more highly solvated, in comparison to the monovalent ions discussed above, the SO_4^{2-} ion must necessarily reside deeper within the interfacial region. The presence of SO_4^{2-} there causes a higher degree of water orientation relative to the interface normal, but without the reduction in the depth of oriented water molecules that is observed for the monovalent anions when the field is screened by the presence of these ions. These two factors would result in an increase in VSFS intensity throughout the spectral region as observed.

Conclusions

The interplay between water and organic molecules creates a unique environment for the ionic adsorption and potential transport across such an interface. Recent studies have found that it also provides a unique platform for enhancing chemical reactions^{53,54} giving further motivation to strive for a greater understanding of this interfacial environment. This study provides a major step toward that knowledge by experimentally probing simple inorganic salt solutions (NaCl , NaBr , NaNO_3 , and Na_2SO_4) adjacent to a hydrophobic liquid CCl_4 . Through surface specific spectroscopic measurements, the nature of the adsorption of these ions at a hydrophobic liquid–aqueous solution interface and their effects on interfacial molecular structure is examined.

Through analysis of the vibrational spectra of interfacial water, comprised of collections of modes of water molecules in varied hydrogen bonding environments and also different locations within the interface, a molecular picture can be derived as to how ions in the salt solution adjacent to the organic liquid

interact, and what impact they have on interfacial molecular properties. These studies provide evidence for the existence of anions not only in the bulk salt solution but also within the interfacial region. Their presence is found to alter the interfacial molecular behavior of water and interfacial properties in a manner that is consistent with the emerging view of the structure of liquid–liquid interfaces that has been derived in our previous VSFS experimental and MD simulation studies.

The experimental results reported in this paper are in stark contrast to what has been obtained in previous VSFS studies of salt solutions in contact with air from our laboratory and others. Reasons for the differing spectral trends for the same bulk concentrations of the same ions lie in the unique nature of the weak interaction between the organic and water phases that influences the adsorption and behavior of ions within the liquid–liquid interface. This interaction results in an average net orientation of the water molecules' dipoles, such that an electric field is created across this very narrow region of the interface. This field, which also causes orienting of the nearby organic liquid, promotes the existence of ions within the region of the interface. For the monovalent anions studied, Cl^- , Br^- , and NO_3^- , the accumulation of the ions into the interfacial region screens the field, previously present at the neat interface, causing a reduction of the orienting force on interfacial water molecules and a narrower interfacial region. For SO_4^{2-} , the tendency to remain highly solvated deeper in the interfacial region causes an increase in water orientation that results in behavior that departs from that of the other ions studied.

The results of these spectroscopic studies provide a bridge between the growing fields of water at hydrophobic surfaces and ions at aqueous surfaces. In particular, they illuminate the importance of the non-aqueous phase and the roles that polarizability, charge, and polarity of this phase will all play in the adsorption and interaction of ions within the interfacial region. Understanding the importance of how the ions respond not only to the surrounding solvating water molecules but also to the forces present from the non-aqueous moieties has important implications in many processes including ion transport across a membrane, groundwater contaminated by organic solvents, and even chemical assembly and synthesis at organic–water interfaces—all of which involve interfaces where a hydrophobic or non-polar phase is adjacent to an ionic aqueous medium.

Acknowledgment. The authors wish to thank the Office of Naval Research for instrumentation and the National Science Foundation (Grant CHE-0652531) for support of this research.

References and Notes

- (1) Beildeck, C. L.; Liu, M. J.; Brindza, M. R.; Walker, R. A. *J. Phys. Chem. B* **2005**, *109*, 14604.
- (2) Charreteur, K.; Quentel, F.; Elleouet, C.; L'Her, M. *Anal. Chem.* **2008**, *80*, 5065.
- (3) Chen, X.; Yang, T.; Kataoka, S.; Cremer, P. S. *J. Am. Chem. Soc.* **2007**, *129*, 12272.
- (4) Laforge, F. O.; Sun, P.; Mirkin, M. V. *J. Am. Chem. Soc.* **2006**, *128*, 15019.
- (5) Luo, G. M.; Malkova, S.; Yoon, J.; Schultz, D. G.; Lin, B. H.; Meron, M.; Benjamin, I.; Vanysek, P.; Schlossman, M. L. *Science* **2006**, *311*, 216.
- (6) Luo, G. M.; Malkova, S.; Yoon, J.; Schultz, D. G.; Lin, B. H.; Meron, M.; Benjamin, I.; Vanysek, P.; Schlossman, M. L. *J. Electroanal. Chem.* **2006**, *593*, 142.
- (7) McArthur, E. A.; Eisenthal, K. B. *J. Am. Chem. Soc.* **2006**, *128*, 1068.
- (8) McFearin, C. L.; Beaman, D. K.; Moore, F. G.; Richmond, G. L. *J. Phys. Chem. C* **2009**, *113*, 1171.
- (9) Moore, F. G.; Richmond, G. L. *Acc. Chem. Res.* **2008**, *41*, 739.
- (10) Shen, Y. R. *Proc. Natl. Acad. Sci. U.S.A.* **1996**, *93*, 12104.

- (11) Benjamin, I. *Science* **1993**, 261, 1558.
(12) Chorny, I.; Benjamin, I. *J. Phys. Chem. B* **2005**, 109, 16455.
(13) Fernandes, P. A.; Cordeiro, M. N. D. S.; Gomes, J. A. N. F. *J. Phys. Chem. B* **2001**, 105, 981.
(14) Frank, S.; Schmickler, W. *J. Electroanal. Chem.* **2006**, 590, 138.
(15) Hore, D. K.; Walker, D. S.; MacKinnon, L.; Richmond, G. L. *J. Phys. Chem. C* **2007**, 111, 8832.
(16) Hore, D. K.; Walker, D. S.; Richmond, G. L. *J. Am. Chem. Soc.* **2008**, 130, 1800.
(17) Schnell, B.; Schurhammer, R.; Wipff, G. *J. Phys. Chem. B* **2004**, 108, 2285.
(18) Su, B.; Eugster, N.; Girault, H. H. *J. Electroanal. Chem.* **2005**, 577, 187.
(19) Wardle, K. E.; Henderson, D. J.; Rowley, R. L. *Fluid Phase Equilib.* **2005**, 233, 96.
(20) Wick, C. D.; Dang, L. X. *Chem. Phys. Lett.* **2008**, 458, 1.
(21) Ghosal, S.; Hemminger, J. C.; Bluhm, H.; Mun, B. S.; Hebenstreit, E. L. D.; Ketteler, G.; Ogletree, D. F.; Requejo, F. G.; Salmeron, M. *Science* **2005**, 307, 563.
(22) Ishiyama, T.; Morita, A. *J. Phys. Chem. C* **2007**, 111, 738.
(23) Jungwirth, P.; Tobias, D. J. *Chem. Rev.* **2006**, 106, 1259.
(24) Jungwirth, P.; Winter, B. *Annu. Rev. Phys. Chem.* **2008**, 59, 343.
(25) Noah-Vanhoucke, J.; Smith, J. D.; Geissler, P. L. *Chem. Phys. Lett.* **2009**, 470, 21.
(26) Pegram, L. M.; Record, M. T. *J. Phys. Chem. B* **2007**, 111, 5411.
(27) Petersen, P. B.; Saykally, R. J. *Annu. Rev. Phys. Chem.* **2006**, 57, 333.
(28) Raymond, E. A.; Richmond, G. L. *J. Phys. Chem. B* **2004**, 108, 5051.
(29) Schnitzer, C.; Baldelli, S.; Shultz, M. J. *J. Phys. Chem. B* **2000**, 104, 585.
(30) Tarbuck, T. L.; Ota, S. T.; Richmond, G. L. *J. Am. Chem. Soc.* **2006**, 128, 14519.
(31) Tarbuck, T. L.; Richmond, G. L. *J. Am. Chem. Soc.* **2006**, 128, 3256.
(32) Lambert, A. G.; Davies, P. B.; Neivandt, D. J. *Appl. Spectrosc. Rev.* **2005**, 40, 103.
(33) McGilp, J. F. *J. Phys. D: Appl. Phys.* **1996**, 29, 1812.
(34) Shen, Y. R. *Principles of nonlinear optics*; John Wiley & Sons: New York, 1984.
(35) Aveyard, R.; Saleem, S. M. *J. Chem. Soc., Faraday Trans.* **1976**, 72.
(36) Bian, H. T.; Feng, R. R.; Xu, Y. Y.; Guo, Y.; Wang, H. F. *Phys. Chem. Chem. Phys.* **2008**, 10, 4920.
(37) Levering, L. M.; Sierra-Hernandez, M. R.; Allen, H. C. *J. Phys. Chem. C* **2007**, 111, 8814.
(38) Scatena, L. F.; Richmond, G. L. *J. Phys. Chem. B* **2001**, 105, 11240.
(39) Bain, C. D.; Davies, P. B.; Ong, T. H.; Ward, R. N.; Brown, M. A. *Langmuir* **1991**, 7, 1563.
(40) Walker, D. S.; Moore, F. G.; Richmond, G. L. *J. Phys. Chem. C* **2007**, 111, 6103.
(41) Walker, D. S.; Richmond, G. L. *J. Am. Chem. Soc.* **2007**, 129, 9446.
(42) Morita, A.; Hynes, J. T. *Chem. Phys.* **2000**, 258, 371.
(43) Gragson, D. E.; Richmond, G. L. *J. Phys. Chem. B* **1998**, 102, 3847.
(44) Jungwirth, P.; Tobias, D. J. *J. Phys. Chem. B* **2001**, 105, 10468.
(45) Ji, N.; Ostroverkhov, V.; Tian, C. S.; Shen, Y. R. *Phys. Rev. Lett.* **2008**, 100.
(46) Liu, D.; Ma, G.; Levering, L. M.; Allen, H. C. *J. Phys. Chem. B* **2004**, 108, 2252.
(47) Sovago, M.; Campen, R. K.; Bakker, H. J.; Bonn, M. *Chem. Phys. Lett.* **2009**, 470, 7.
(48) Tian, C. S.; Shen, Y. R. *Chem. Phys. Lett.* **2009**, 470, 1.
(49) Chang, T. M.; Dang, L. X. *J. Chem. Phys.* **1996**, 104, 6772.
(50) Jedlovsky, P.; Vincze, A.; Horvai, G. *Phys. Chem. Chem. Phys.* **2004**, 6, 1874.
(51) Hore, D. K.; Walker, D. S.; Richmond, G. L. *J. Am. Chem. Soc.* **2007**, 129, 752.
(52) Otten, D. E.; Petersen, P. B.; Saykally, R. J. *Chem. Phys. Lett.* **2007**, 449, 261.
(53) Jung, Y. S.; Marcus, R. A. *J. Am. Chem. Soc.* **2007**, 129, 5492.
(54) Narayan, S.; Muldoon, J.; Finn, M. G.; Fokin, V. V.; Kolb, H. C.; Sharpless, K. B. *Angew. Chem., Int. Ed.* **2005**, 44, 3275.

JP906616C